Positive Quantitative Relationship between EMT and Contact-Initiated Sliding on Fiber-like Tracks

Daniel F. Milano,[1] Robert J. Natividad,[2] Yasuhiro Saito,[4] Catherine Y. Luo,[2] Senthil K. Muthuswamy,[4] and Anand R. Asthagiri[1,2,3,*]

[1]Department of Chemical Engineering, [2]Department of Bioengineering, and [3]Department of Biology, Northeastern University, Boston, Massachusetts; and [4]Beth Israel Deaconess Medical Center, Harvard Medical School, Boston, Massachusetts

ABSTRACT Epithelial-mesenchymal transition (EMT) is a complex process by which cells acquire invasive properties that enable escape from the primary tumor. Complete EMT, however, is not required for metastasis: circulating tumor cells exhibit hybrid epithelial-mesenchymal states, and genetic perturbations promoting partial EMT induce metastasis in vivo. An open question is whether and to what extent intermediate stages of EMT promote invasiveness. Here, we investigate this question, building on recent observation of a new invasive property. Migrating cancer cell lines and cells transduced with prometastatic genes slide around other cells on spatially confined, fiberlike micropatterns. We show here that low-dosage/short-duration exposure to transforming growth factor beta (TGFβ) induces partial EMT and enables sliding on narrower (26 μm) micropatterns than untreated counterparts (41 μm). High-dosage/long-duration exposure induces more complete EMT, including disrupted cell-cell contacts and reduced E-cadherin expression, and promotes sliding on the narrowest (15 μm) micropatterns. These results identify a direct and quantitative relationship between EMT and cell sliding and show that EMT-associated invasive sliding is progressive, with cells that undergo partial EMT exhibiting intermediate sliding behavior and cells that transition more completely through EMT displaying maximal sliding. Our findings suggest a model in which fiber maturation and EMT work synergistically to promote invasiveness during cancer progression.

INTRODUCTION

The epithelial-mesenchymal transition (EMT) plays a significant role in cancer progression and is often associated with metastasis and poor prognosis (1–5). EMT is a complex process in which epithelial cells lose expression of epithelial genes, upregulate mesenchymal markers and proteins associated with migration and invasion, and undergo changes in morphology (6–8). It is increasingly evident that EMT can also progress only partially, resulting in hybrid epithelial/mesenchymal (E/M) states in which cells exhibit a mix of epithelial and mesenchymal molecular markers (9–11). Indeed, complete EMT is not absolutely essential for metastasis, as evidenced for example by circulating tumor cells exhibiting partial EMT (12–14).

Hybrid E/M states also occur during the temporal progression of EMT induced by cues, such as transforming growth factor beta (TGFβ). TGFβ is a potent inducer of EMT (15) and promotes gradual changes in cell morphology and gene expression over the course of several days in cul-ture. During this time span, cells exhibit a mix of epithelial and mesenchymal molecular markers. After 48 h of TGFβ treatment, nontransformed mammary epithelial MCF-10A cells upregulate smooth muscle actin (16). However, an overt EMT, defined by reduced E-cadherin expression, induction of vimentin expression, and a distinct morphology change, required 6 days of sustained exposure to TGFβ. Stable hybrid E/M states have been predicted (17,18) and demonstrated experimentally in MCF-10A cells treated with different doses of TGFβ (19).

Given the prevalence of partial EMT and its significant role in cancer progression, it is important to better understand how cell behaviors associated with metastasis and invasion change as cells progress through the intermediate stages of EMT. As cells switch their molecular expression profile, are there gradual concomitant changes in invasive cell behavior? Do intermediate stages of EMT correspond to intermediate levels of invasive cell behavior that, despite being submaximal, may be quantitatively sufficient for disease progression?

To begin to examine the quantitative relationship between degree of EMT and invasive cell behavior, we investigate here the effect of TGFβ-induced EMT on a cell migration

phenotype that is relevant to invasion in a fibrillar, crowded tumor microenvironment and that we recently demonstrated to be correlated with metastasis (20). Cancer cells invade along fibers in a highly dynamic microenvironment with a high concentration of cells (21–23). How invading cancer cells respond to encounters with other cells along their migratory path will influence the efficiency of cancer cell dispersion. A cell that halts and reverses direction at every cell-cell encounter has a lower rate of dispersion compared to a cell that circumnavigates or slides around other cells to maintain its direction of movement.

We recently showed that metastatic MDA-MB-231 and BT-549 cells are highly effective in sliding around cell-cell encounters on fiberlike adhesive tracks, even on tracks much narrower than the cell diameter (20). In contrast, non-transformed mammary epithelial MCF-10A cells largely reverse direction upon encountering another cell. Corroborating the relationship between contact-initiated sliding and invasive potential, molecular perturbations associated with cancer progression, including treatment with TGFβ, downregulation of E-cadherin and PARD3 tumor suppressors, and ErbB2 induction, enhanced sliding behavior in MCF-10A cells.

To what extent EMT is involved in promoting sliding behavior is unclear. Extended treatment with a high dose of TGFβ promotes EMT and enhances sliding behavior of MCF-10A cells (20). On the other hand, without inducing overt EMT, downregulation of PARD3 alongside induction of ErbB2 signaling enhanced sliding and induced metastasis in mouse models. These observations suggest that complete EMT is not required for sliding, and pose the hypothesis that the degree of EMT quantitatively affects the extent of invasive sliding behavior.

Here, we sought to test this hypothesis and investigate the quantitative relationship between EMT and contact-initiated sliding. We used different doses and durations of TGFβ treatment to modulate the extent of EMT and measured the corresponding ability of cells to undergo slide responses on spatially confined, fiberlike micropatterns. Our results show that the acquisition of invasive sliding behavior is progressive and correlates with the extent of TGFβ-induced EMT. These results suggest a model wherein the extent of EMT cooperates with fiber maturation to promote an invasive phenotype during cancer progression.

MATERIALS AND METHODS

Micropatterning and surface preparation

Fiberlike micropatterned surfaces were prepared and seeded as described in Milano et al. (20). Briefly, fibronectin was adsorbed on poly(dimethylsiloxane) elastomeric stamps containing negative relief features and then transferred to a plasma-treated poly(dimethylsiloxane) spin-coated glass surfaces with high spatial control. Patterned surfaces were visualized via fluorescence microscopy by copatterning trace Alex Fluor 594-conjugated BSA (Invitrogen, Carlsbad CA). Before cell seeding, surfaces were incu-

bated with Pluronic F127 (EMD Biosciences, San Diego CA) to prevent nonspecific cell adhesion. TGFβ-treated and untreated MCF-10A cells were seeded on the surface at a density of 2.0×10^4 cells/mL and incubated for ~1 h. Nonadhered cells were gently removed via consecutive PBS washes before the remaining adhered cells in the dish were given fresh growth media and the dish was transferred to the microscope for imaging.

Image acquisition and analysis

Dishes were secured on a heated microscope stage maintained at 37°C and 5% CO_2. Individual positions were specified as x,y,z coordinates in Axiovision or Zen software (Carl Zeiss, Göttingen, Germany). Phase contrast images of every position were acquired at 5-min intervals for 21 h at 10× magnification on an Axiovert 200M or LSM 700 confocal microscope (Carl Zeiss). Frame-by-frame image analysis was performed with the software Fiji (National Institutes of Health, Bethesda, MD; open-access). Instances where two cells are observed to make contact are followed over time until the cells come apart. The pairwise collision is recorded as a slide if the cells circumnavigated each other and continued to move along their original trajectory; meanwhile, if the cells interacted and reversed direction, the collision event was scored as a reversal.

Cell culture

Nontransformed mammary epithelial MCF-10A cells were transfected with a double reporter to express GFP-tagged H2B and mCherry-tagged GM130 proteins as described in Wang et al. (24). Cells were maintained using standard MCF-10A cell culture methods, as described in Kushiro and Asthagiri (25). To induce EMT, the growth medium was supplemented with TGFβ (PeproTech, Rocky Hill, NJ). Two doses of TGFβ were analyzed: 5 and 20 ng/mL. The duration of TGFβ treatment ranged from 3 to 12 days. During extended treatments (>3 days), treated cells were passaged regularly and provided with fresh TGFβ-supplemented growth medium.

Western blot

E-cadherin was probed using a 1:1000 dilution of primary antibodies (Santa Cruz Biotechnology, Santa Cruz, CA) and a 1:1500 dilution of HRP-conjugated secondary antibody (Thermo Fisher Scientific, Waltham, MA). N-cadherin was probed using a 1:1000 dilution of primary antibody (No. 13116; Cell Signaling Technology, Danvers, MA) and a 1:10,000 dilution of HRP-conjugated secondary antibody (NA934V; GE Healthcare, Marlborough, MA). Erk2 was probed using a 1:200 dilution of primary antibody (Santa Cruz Biotechnology) and a 1:100,000 dilution of HRP-conjugated secondary antibody (Thermo Fisher Scientific). Western blots were imaged by ECL (Thermo Fisher Scientific) using a ChemiDoc Touch Imaging System (BioRad, Hercules, CA). Quantification of the blot by densitometry was performed in Image Lab (BioRad).

Data analysis and statistics

Data analysis and statistics were conducted in MATLAB (The Mathworks, Natick MA) and with the statistical analysis software R (GNU Project).

RESULTS AND DISCUSSION

The extent of EMT induced by TGFβ depends on dose and duration of treatment

To model cells at different stages of EMT, nontransformed mammary epithelial MCF-10A cells were exposed to either a low (5 ng/mL) or high (20 ng/mL) dose of TGFβ 1

(Peprotech) for up to 12 days. Cells were passaged at 3-day intervals as described in Roussos et al. (22) and provided with fresh TGFβ.

Cells exposed to the high dose of TGFβ undergo a morphology change before 3 days of treatment (Fig. 1 *I*, *asterisks*). Meanwhile, cells treated with the low 5 ng/mL dose required 6 days to demonstrate the same elongated, spindle-shape morphology consistent with EMT (Fig. 1 *F*, *asterisks*). Cell-cell contacts in the high 20 ng/mL dose cohort were poorly defined by day 6 and persisted through day 12 (Fig. 1 *L*, *arrowheads*). Although cells treated with the low dose undergo a morphology change, contacts between these cells remained intact throughout the entire 12-day duration of treatment (Fig. 1, *G* and *H*). Control cells that were not exposed to TGFβ maintained the cobblestone morphology characteristic of epithelial cells (Fig. 1, *A–D*). These qualitative changes in cell morphology were confirmed by quantitation: TGFβ treatment increased the shape factor of cells, indicative of greater deviation from a rounded shape, and increased the void space between cells, consistent with a loss of cell-cell contacts (see Fig. S1 and Table S1 in the Supporting Material). Taken together, these findings show that TGFβ induces a gradual progression from an epithelial to mesenchymal morphology in a dosage- and time-dependent manner.

To corroborate observed changes in morphology, we examined molecular-level changes in the expression of E-cadherin and N-cadherin, both well-established markers of the epithelial and mesenchymal states, respectively. Western blotting showed that E-cadherin expression level decreased (Fig. 2 *A*) and N-cadherin expression level increased (Fig. S2) with time after exposure to TGFβ. Quantifying the changes in E-cadherin expression showed that E-cadherin expression decreases gradually over time after TGFβ treatment (Fig. 2 *B*). Both doses of TGFβ triggered downregulation of E-cadherin, with the higher dose of TGFβ having a quicker effect. Thus, similar to morphological changes, the extent of gene expression changes associated with EMT depends on the dose and duration of TGFβ exposure, with the cell population expressing both epithelial and mesenchymal markers concomitantly at some time points.

TGFβ-treated MCF-10A cells slide more efficiently than untreated cells

We next asked how different stages of progression along the TGFβ-induced EMT pathway affect invasive cell sliding behavior. Pairwise interactions between migrating cells with and without TGFβ treatment were imaged and the extent to which interacting cells reversed direction versus sliding past each other was quantified as described in Milano et al. (20).

Untreated cells are unable to slide effectively on narrow and intermediate line widths (6–21 μm) (Fig. 3 *A*). On broader line widths, untreated cells begin to exhibit a
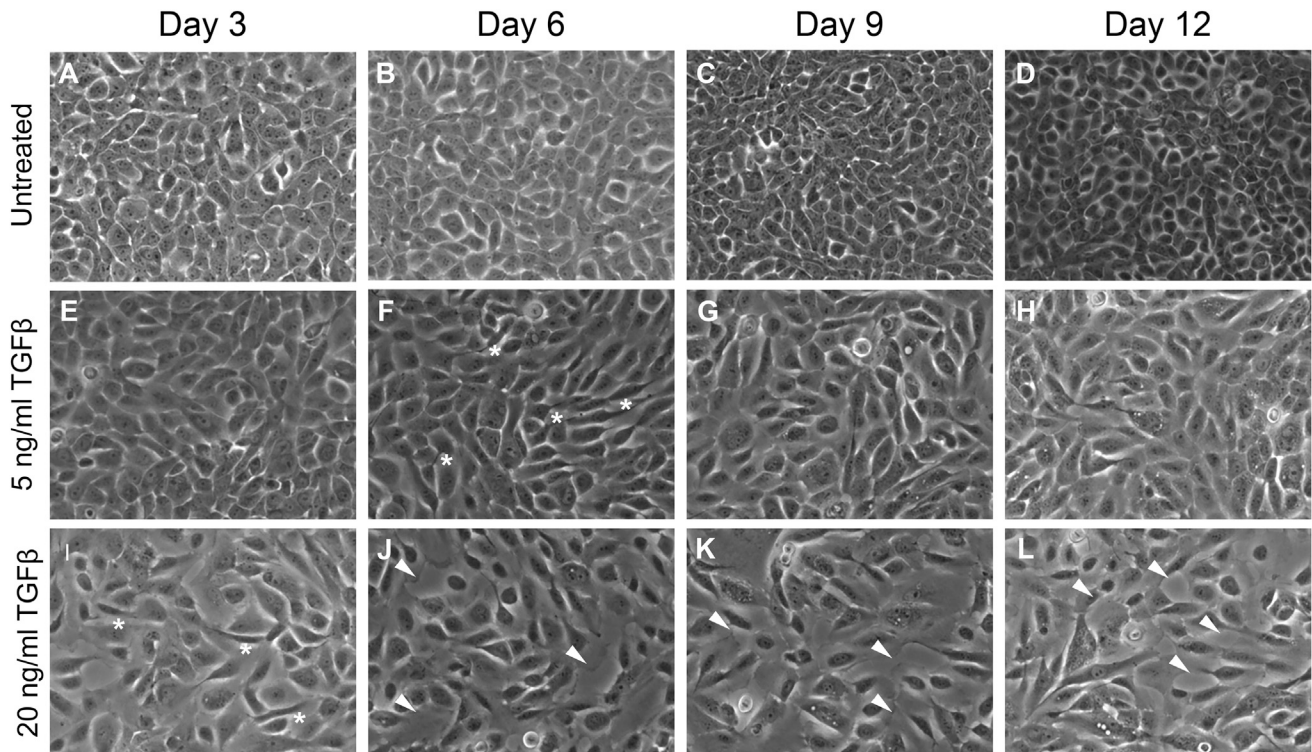

FIGURE 1 (*A–L*) Cell morphology changes induced by TGFβ treatment. Nontransformed mammary epithelial MCF-10A cells were treated with TGFβ or left untreated. Treated cells were exposed to either 5 or 20 ng/mL of TGFβ for between 3 and 12 days. (*Asterisks*) Cells with an elongated, mesenchymal morphology. (*Arrowheads*) Deficient cell-cell adhesions. Phase contrast images were taken before cell passage at 10× magnification.
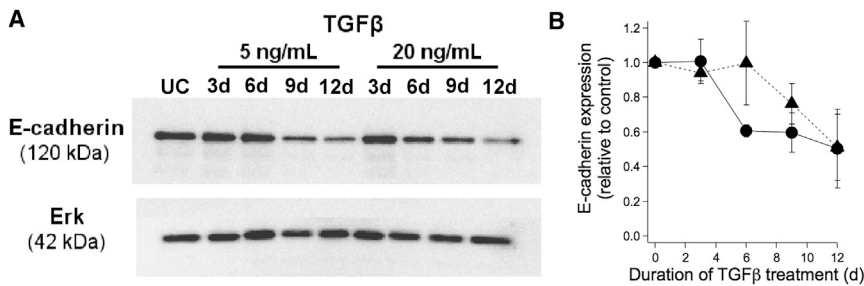
A

B

FIGURE 2 Extent of TGFβ-induced EMT. (*A*) E-cadherin expression was measured by Western blot in TGFβ-treated and untreated (control) cells. Erk2 was probed as an equal-loading control. (*B*) Quantification of the ratio of E-cadherin/Erk expression for cells treated with 5 ng/mL (*triangle*) or 20 ng/mL (*circle*) TGFβ. Values are reported relative to the E-cadherin/Erk expression ratio for untreated cells. Two-way ANOVA indicates that the dependence of E-cadherin expression on time of exposure is statistically significant ($p < 0.05$), whereas the effect of dose is not statistically distinguishable. Error bars denote SD.

modest level of sliding, with sliding observed in 20% of collisions at the broadest 33-μm micropattern width. These results are consistent with our previous findings showing a limited ability of nontransformed cells to undergo invasive contact-initiated slide responses.
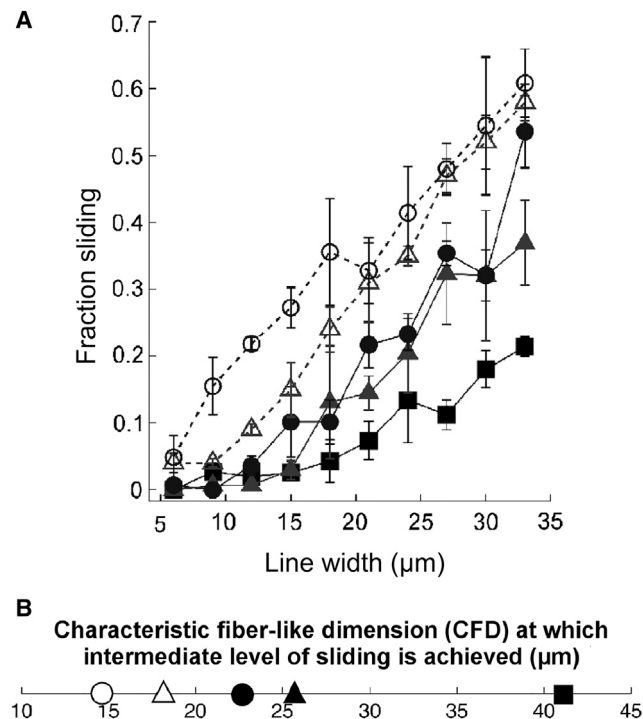

FIGURE 3 Collision response as a function of TGFβ treatment. (*A*) Fraction sliding and (*B*) CFD for TGFβ-treated and untreated (control, *square*) cells. MCF-10A cells were treated with either 5 ng/mL TGFβ (*triangle*) for three days (*solid representation, solid line*) or six days (*open, dashed line*); and 20 ng/mL TGFβ (*circle*) for three days (*solid representation, solid line*) or 12 days (*open, dashed line*). In total, 7226 cell-cell collisions were analyzed across all 50 combinations of five TGFβ treatment conditions and 10 micropattern widths (detailed breakdown of sample sizes provided in Table S2). For each TGFβ treatment condition, including control, the dependence of fraction sliding on line width is statistically significant ($p < 0.001$). Meanwhile, the dependence of fraction sliding on TGFβ treatment was statistically significant at line widths of 12 μm ($p < 0.001$) and 9, 15, 21, 27, and 33 μm ($p < 0.05$). The dependence of fraction sliding on TGFβ treatment at line widths of 6, 18, 24, and 30 μm were not statistically significant. Further details on analysis of variance are provided in the Supporting Material. Error bars denote mean ± SE.

Treatment with TGFβ enhances contact-initiated sliding in a manner that depends on the dose of TGFβ, the duration of TGFβ exposure, and the micropattern width. At the higher range of micropattern widths (24–33 μm), even the shortest exposure (3 day) and lowest dose (5 ng/mL) of TGFβ increases the fraction of collisions that result in sliding. Treatment with either 5 ng/mL or 20 ng/mL TGFβ for 3 days generated similar levels of sliding. Meanwhile, increasing exposure time to 6 and 12 days for 5 ng/mL and 20 ng/mL doses of TGFβ, respectively, further increased the level of sliding. Thus, the duration of exposure has a larger effect than TGFβ dose on wide micropatterns. At the lower line widths (6–18 μm), short exposures of 3 days to TGFβ only modestly enhanced sliding behavior, if at all. Extended duration of exposure (6–12 d) was needed to substantially increase sliding behavior.

Notably, given a high TGFβ dose (20 ng/mL) and extended exposure (12 days), sliding was observed in nearly 20% of collisions on narrow 9-μm line widths. For comparison, this level of sliding was observed in untreated cells only when micropatterns were widened to ≥ 30 μm.

To better quantify how TGFβ-induced EMT enhances cell sliding under spatial constraints, we determined the characteristic fiberlike dimension (CFD) at which cells exhibit an intermediate level of sliding. We previously demonstrated that the CFD is an effective metric for quantifying the effects of molecular perturbations on the sliding ability of nontransformed and metastatic breast epithelial cells (20). Cells that slide poorly have a high CFD and require much wider fiberlike tracks to execute moderate levels of sliding; in contrast, cells that slide proficiently have a low CFD and achieve moderate levels of sliding at low fiberlike dimensions. Because the fraction of collisions that exhibit a sliding response varied between 0% and a maximum of ~50–60% (Fig. 3 *A*), we set the intermediate level of sliding to be 25%. Using a linear fit, we determine the CFD at which 25% of collisions result in a sliding response (Fig. S3).

Untreated (control) cells have a CFD of 41 μm (Fig. 3 *B*). Cells exposed to 5 ng/mL of TGFβ for 3 days have a lower CFD of 26 μm, indicating an enhanced ability to slide in confined environments. Extending 5 ng/mL TGFβ exposure to 6 days further reduces the CFD to 18 μm, corresponding with the acquisition of a more elongated morphology

(Fig. 1). This progressive reduction in CFD with further progression along the EMT pathway is also observed at the higher TGFβ dose. At 20 ng/mL TGFβ for 3 days, cells exhibit an elongated morphology and the CFD of 23 μm is lower than the untreated control. Extending the exposure to 12 days when cell-cell contacts are compromised (Fig. 1, *white arrowheads*), the CFD drops even further to 15 μm.

Dose-dependent kinetics of E-cadherin downregulation reveals two modes by which TGFβ enhances sliding behavior

We next investigated the relationship between the progressive enhancement in cell sliding behavior and the changes in E-cadherin expression level. We have previously shown that downregulating E-cadherin using shRNA constructs enhances sliding and reduces CFD in MCF-10A cells; meanwhile, overexpressing E-cadherin in metastatic MDA-MB-231 cells inhibits sliding and increases CFD (20). Therefore, we hypothesized that the progressive enhancement in cell sliding during EMT may correspond quantitatively with concomitant decreases in E-cadherin expression.

The quantitative relationship between E-cadherin expression and cell sliding behavior across the different TGFβ treatments and the untreated control revealed two regimes (Fig. 4). Cells treated with 5 ng/mL TGFβ for 3 and 6 days and 20 ng/mL TGFβ for 3 days have approximately the same level of E-cadherin expression as untreated controls. Yet, the CFD and sliding behavior are significantly different among these conditions. We conclude that in this regime of EMT, molecular changes independent of E-cadherin are mechanistically involved in enhancing cell-sliding behavior. In contrast, in the second regime of EMT where 20 ng/mL TGFβ is applied for 12 d, E-cadherin expression decreases by ~50% and corresponds to a reduction in CFD
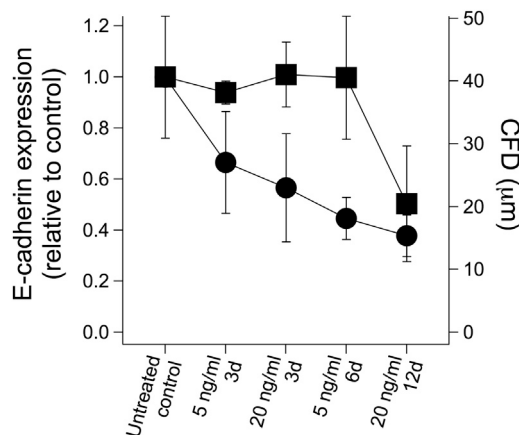

FIGURE 4 TGFβ-induced EMT promotes two regimes of invasive behavior. E-cadherin expression (*solid squares*, *left y axis*) and CFD values (*solid circles*, *right y axis*) are plotted for cells left untreated or treated with different doses and durations of TGFβ (*x axis*). Error bars denote SD for E-cadherin expression and the 95% confidence interval for CFD.

and enhancement in cell sliding. In this portion of the EMT process, the loss of E-cadherin expression is correlated with an increase in the ability of cells to undergo contact-initiated sliding. Taken together, these results help to identify segments of the complex EMT process in which cell sliding behavior is enhanced independent of E-cadherin regulation and other segments in which downregulation of E-cadherin may facilitate cell sliding.

Our data suggest E-cadherin-independent mechanisms may be involved in EMT-mediated enhancement of sliding. For example, EMT is known to disrupt apical-basal polarity (26). We previously showed that an apically localized regulator of cell polarity, PAR3, modulates cell sliding (20). In addition, we observe that N-cadherin expression increases after 6 d treatment with 5 ng/mL TGFβ (Fig. S2), a condition at which E-cadherin levels remain unaffected (Fig. 2). Increased N-cadherin, even in the presence of E-cadherin, has been reported to enhance breast epithelial cell motility and invasiveness (27). It is also formally possible that TGFβ may regulate sliding through pathways parallel to EMT. Our data suggest that if pathways parallel to EMT are involved, they must evolve over many days, similar to the protracted kinetics of EMT progression, and are likely to involve changes in gene expression.

CONCLUSIONS

We report three main insights into the quantitative relationship between EMT and invasive cell sliding behavior. First, there is a strong positive relationship between EMT and the sliding phenotype. When cells have progressed into EMT under maximal stimulation (20 ng/mL TGFβ for 12 days), the CFD drops to 15 μm. For comparison, we previously reported a CFD of 10 μm for triple-negative, claudin-low BT549 cells (20). Thus, exposing an otherwise noninvasive epithelial MCF-10A cell to 20 ng/mL of TGFβ for 12 days is sufficient to induce an invasive phenotype on par with highly metastatic breast cancer cells. Second, mesenchymal transition enables cells to slide under extremely tight spatial constraints. The CFD of 15 μm under maximal TGFβ treatment is 2.7-fold narrower than the CFD of 41 μm for untreated control cells. To put this physical restriction in perspective, a CFD of 15 μm is comparable to the diameter of a single MCF-10A cell. Finally, partial progression through EMT leads to intermediate levels of invasive cell sliding behavior. Submaximal treatment with TGFβ using reduced dose and/or shorter duration of exposure promotes partial changes in cell morphology while concomitantly reducing CFD. The shift in CFD from 41 μm for untreated cells to 15 μm under maximal TGFβ stimulation is not a switchlike transformation but rather occurs through progressive shifts in sliding ability under ever tighter spatial constraints. These findings suggest a model in which fiber maturation and partial EMT work synergistically to promote invasiveness during cancer progression.

Milano et al.

SUPPORTING MATERIAL

Supporting Materials and Methods, three figures, and two tables are available at http://www.biophysj.org/biophysj/supplemental/S0006-3495(16)30759-7.

AUTHOR CONTRIBUTIONS

D.F.M., S.K.M., and A.R.A. conceived and designed the experiments; D.F.M., R.N., and Y.S. performed the experiments; and D.F.M., R.N., Y.S., C.Y.L., and A.R.A. analyzed the results and wrote the article. All authors edited the article.

ACKNOWLEDGMENTS

REFERENCES

1. Brabletz, T. 2012. EMT and MET in metastasis: where are the cancer stem cells? *Cancer Cell.* 22:699–701.

2. Chaffer, C. L., and R. A. Weinberg. 2011. A perspective on cancer cell metastasis. *Science.* 331:1559–1564.

3. Guarino, M., B. Rubino, and G. Ballabio. 2007. The role of epithelial-mesenchymal transition in cancer pathology. *Pathology.* 39:305–318.

4. Thiery, J. P. 2002. Epithelial-mesenchymal transitions in tumour progression. *Nat. Rev. Cancer.* 2:442–454.

5. Thiery, J. P., H. Acloque, …, M. A. Nieto. 2009. Epithelial-mesenchymal transitions in development and disease. *Cell.* 139:871–890.

6. Onder, T. T., P. B. Gupta, …, R. A. Weinberg. 2008. Loss of E-cadherin promotes metastasis via multiple downstream transcriptional pathways. *Cancer Res.* 68:3645–3654.

7. Vuoriluoto, K., H. Haugen, …, J. Ivaska. 2011. Vimentin regulates EMT induction by Slug and oncogenic H-Ras and migration by governing Axl expression in breast cancer. *Oncogene.* 30:1436–1448.

8. Xie, L., B. K. Law, …, H. L. Moses. 2004. Activation of the Erk pathway is required for TGF-β1-induced EMT in vitro. *Neoplasia.* 6:603–610.

9. Hollestelle, A., J. K. Peeters, …, J. W. Martens. 2013. Loss of E-cadherin is not a necessity for epithelial to mesenchymal transition in human breast cancer. *Breast Cancer Res. Treat.* 138:47–57.

10. Huang, R. Y., M. K. Wong, …, J. P. Thiery. 2013. An EMT spectrum defines an anoikis-resistant and spheroidogenic intermediate mesenchymal state that is sensitive to e-cadherin restoration by a src-kinase inhibitor, saracatinib (AZD0530). *Cell Death Dis.* 4:e915.

11. Sarrio, D., C. K. Franklin, …, C. M. Isacke. 2012. Epithelial and mesenchymal subpopulations within normal basal breast cell lines exhibit distinct stem cell/progenitor properties. *Stem Cells.* 30:292–303.

12. Armstrong, A. J., M. S. Marengo, …, M. A. Garcia-Blanco. 2011. Circulating tumor cells from patients with advanced prostate and breast cancer display both epithelial and mesenchymal markers. *Mol. Cancer Res.* 9:997–1007.

13. Grosse-Wilde, A., A. Fouquier d'Hérouël, …, S. Huang. 2015. Stemness of the hybrid epithelial/mesenchymal state in breast cancer and its association with poor survival. *PLoS One.* 10:e0126522.

14. Yu, M., A. Bardia, …, S. Maheswaran. 2013. Circulating breast tumor cells exhibit dynamic changes in epithelial and mesenchymal composition. *Science.* 339:580–584.

15. Massagué, J. 2008. TGFβ in cancer. *Cell.* 134:215–230.

16. Brown, K. A., M. E. Aakre, …, H. L. Moses. 2004. Induction by transforming growth factor-β1 of epithelial to mesenchymal transition is a rare event in vitro. *Breast Cancer Res.* 6:R215–R231.

17. Lu, M., M. K. Jolly, …, E. Ben-Jacob. 2013. MicroRNA-based regulation of epithelial-hybrid-mesenchymal fate determination. *Proc. Natl. Acad. Sci. USA.* 110:18144–18149.

18. Tian, X. J., H. Zhang, and J. Xing. 2013. Coupled reversible and irreversible bistable switches underlying TGFβ-induced epithelial to mesenchymal transition. *Biophys. J.* 105:1079–1089.

19. Zhang, J., X. J. Tian, …, J. Xing. 2014. TGF-β-induced epithelial-to-mesenchymal transition proceeds through stepwise activation of multiple feedback loops. *Sci. Signal.* 7:ra91.

20. Milano, D. F., N. A. Ngai, …, A. R. Asthagiri. 2016. Regulators of metastasis modulate the migratory response to cell contact under spatial confinement. *Biophys. J.* 110:1886–1895.

21. Provenzano, P. P., K. W. Eliceiri, …, P. J. Keely. 2006. Collagen reorganization at the tumor-stromal interface facilitates local invasion. *BMC Med.* 4:38.

22. Roussos, E. T., M. Balsamo, …, J. S. Condeelis. 2011. Mena invasive (MenaINV) promotes multicellular streaming motility and transendothelial migration in a mouse model of breast cancer. *J. Cell Sci.* 124:2120–2131.

23. Wang, W., J. B. Wyckoff, …, J. S. Condeelis. 2002. Single cell behavior in metastatic primary mammary tumors correlated with gene expression patterns revealed by molecular profiling. *Cancer Res.* 62:6278–6288.

24. Wang, H., S. Lacoche, …, S. K. Muthuswamy. 2013. Rotational motion during three-dimensional morphogenesis of mammary epithelial acini relates to laminin matrix assembly. *Proc. Natl. Acad. Sci. USA.* 110:163–168.

25. Kushiro, K., and A. R. Asthagiri. 2012. Modular design of micropattern geometry achieves combinatorial enhancements in cell motility. *Langmuir.* 28:4357–4362.

26. Lamouille, S., J. Xu, and R. Derynck. 2014. Molecular mechanisms of epithelial-mesenchymal transition. *Nat. Rev. Mol. Cell Biol.* 15:178–196.

27. Nieman, M. T., R. S. Prudoff, …, M. J. Wheelock. 1999. N-cadherin promotes motility in human breast cancer cells regardless of their E-cadherin expression. *J. Cell Biol.* 147:631–644.

Supplemental Information

Positive Quantitative Relationship between EMT and Contact-Initiated Sliding on Fiber-like Tracks

Daniel F. Milano, Robert J. Natividad, Yasuhiro Saito, Catherine Y. Luo, Senthil K. Muthuswamy, and Anand R. Asthagiri

Supplemental Information

1. Quantification of TGFß-mediated morphological changes

Contours of the bodies of cells treated with different doses and duration of TGFß were manually outlined using Photoshop. Void regions where no cells were present were also outlined. Properties of these contoured regions-of-interest (ROI) were quantified using Matlab. From ROIs associated with cell bodies, the perimeter and area were quantified, and the shape factor was calculated as the Perimeter^2/(4π Area). A circle has a shape factor of 1, and shapes deviating from a circle have a shape factor greater than 1. Supplemental Table 1 summarizes the shape factor for cells left untreated or treated with different doses and duration of TGFß.

Treatment	Shape Factor	95% Confidence Interval
UC	1.42	0.08
5 ng/ml (3d)	1.51	0.07
5 ng/ml (6d)	1.63	0.10
20 ng/ml (3d)	1.57	0.11
20 ng/ml (12d)	1.52	0.11

Supplemental Table 1. Cells exhibit a more extended morphology following TGFβ treatment. The shape factor is higher among TGFβ-treated cells compared to untreated controls, consistent with an elongation of the cell body.

From ROIs associated with void regions, the void area was quantified, and the fraction of total surface area that was devoid of cells was calculated. The fold-change in the void fraction is depicted in Supplemental Figure 1. Longer exposure and higher doses of TGFß yielded higher fold-change in void fraction, consistent with the observed loss of cell-cell contacts with greater TGFß treatment.
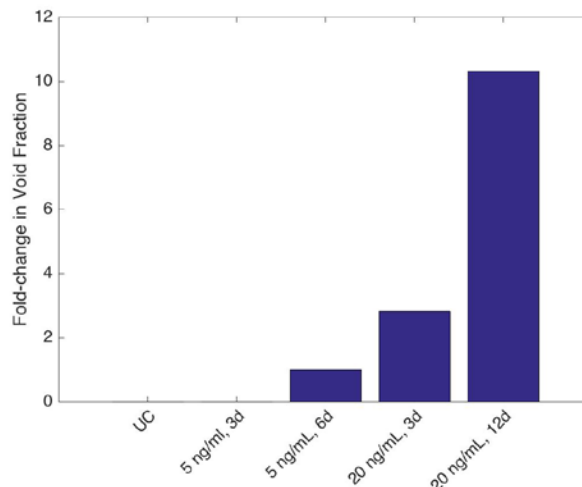

Supplemental Figure 1. Fold-change in void regions between cells. TGFβ-induced EMT results in loss of cell-cell contact. The amount of void areas between cells was quantified from a representative image of cells left untreated or treated with TGFβ at different doses

and duration. The untreated control and treatment with 5 ng/ml TGFβ for 3 d exhibited no void regions. For the other treatment conditions, the void fraction increased with higher exposure time and dose, with cells treated with 20 ng/ml TGFβ for 12 d exhibiting approximately 10-fold greater void regions than those treated with 5 ng/ml TGFβ for 6 d.

2. Upregulation of N-cadherin in response to TGFβ treatment

A characteristic marker of the mesenchymal state is the expression of N-cadherin. We assayed by Western blot the effect of TGFβ-mediated EMT on the expression level of N-cadherin (Supplemental Fig. 2). For both 5 ng/ml and 20 ng/ml of TGFβ, the level of N-cadherin increased gradually with time, and the final steady-state expression level of N-cadherin after 12 h of TGFβ treatment was clearly above the expression level in control untreated cells.
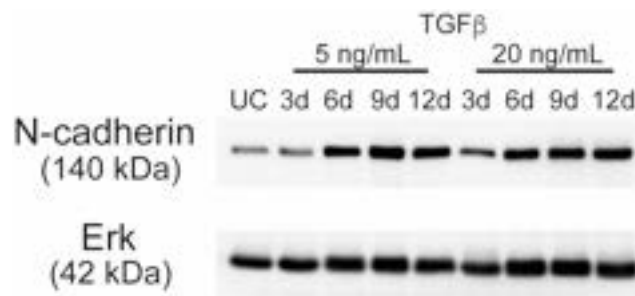
Supplemental Figure 2. N-cadherin expression was measured by Western Blot in TGFβ-treated and untreated (control) cells. Erk2 was probed as an equal-loading control.

3. Number of cell-cell collisions analyzed

In total, 7226 cell-cell encounters were analyzed across 50 combinations of 5 TGFβ treatment and 10 fiber-like micropattern widths. Supplemental Table 2 details the number of cell-cell collisions analyzed at each of the 50 conditions.

| Condition	Width of fiber-like micropattern (µm)										Marginal total
	6	9	12	15	18	21	24	27	30	33	
Untreated	38	74	103	117	117	95	112	125	112	112	1005
TGFβ 5 ng/ml, 3 d	118	159	138	101	84	124	127	102	78	65	1096
TGFβ 5 ng/ml, 6 d	168	202	207	155	185	202	249	211	185	193	1957
TGFβ 20 ng/ml, 3 d	142	133	140	137	138	152	146	127	137	110	1362
TGFβ 20 ng/ml, 12 d	83	129	119	176	177	195	169	202	257	299	1806
Marginal total	549	697	707	686	701	768	803	767	769	779	7226

Supplemental Table 2. Number of collisions analyzed at every combination of ten fiber-like micropattern widths and five TGFβ treatment conditions.

4. Statistical analysis of sliding response

Two-way ANOVA was performed to test the null hypothesis that fraction sliding does not depend on either TGFß treatment or the width of the fiber-like micropattern (data shown in Figure 3A). The analysis was performed using statistical analysis software R (v3.3.1) and shows that fraction sliding exhibits a statistically significant dependence on TGFß treatment ($p < 2e-16$) and line width ($p < 2e-16$). The interaction between these factors is significant ($p < 0.05$); therefore, we conducted detailed analysis of simple effects by 1-way ANOVA, with the Sidak-Bonferroni correction for familywise error. For each TGFß treatment condition, including control, the dependence of fraction sliding on line width was statistically significant ($p < 0.001$). Meanwhile, the dependence of fraction sliding on TGFß treatment was statistically significant at line widths of 12 μm ($p < 0.001$, ***) and 9, 15, 21, 27 and 33 μm ($p < 0.05$, *). The dependence of fraction sliding on TGFß treatment at line widths of 6, 18, 24 and 30 μm were not statistically significant by ANOVA (ns).

5. Characteristic fiber-like dimension (CFD)

We previously defined the CFD as the hypothetical line width required to support moderate sliding (i.e. 25% sliding) on fiber-like micropatterns (20). Here, we applied the same linear model to fraction sliding data for untreated and TGFß-treated MCF-10A cells (Supplemental Fig. 3). Increasing the dose and duration of TGFß treatment progressively reduced the calculated value of the CFD compared to untreated (control) cells.
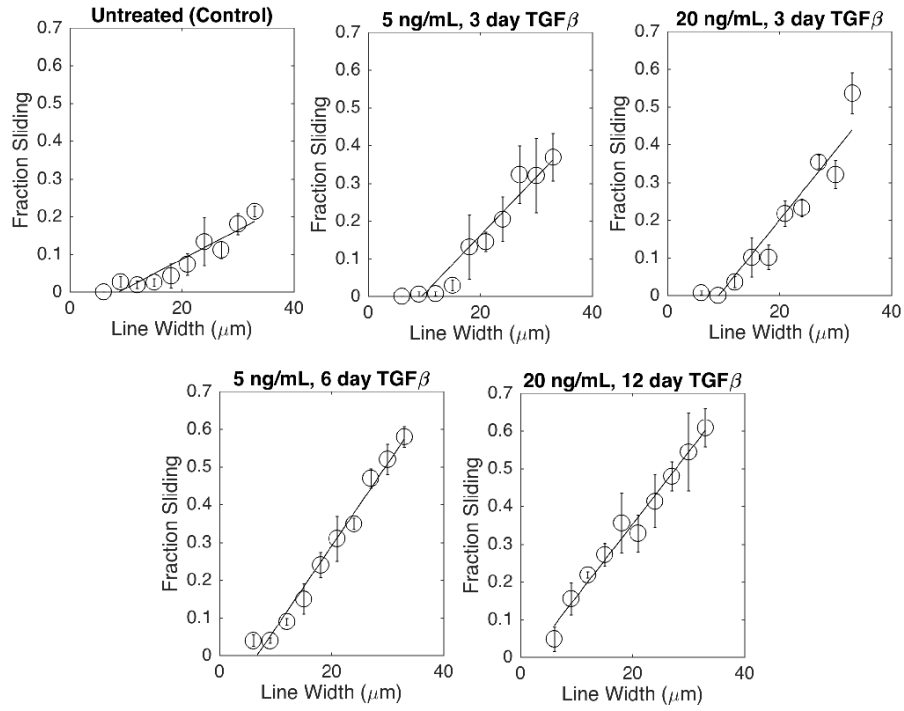
Supplemental Figure 3. A simple linear model was applied to fraction sliding data for untreated and TGFβ-treated MCF-10A cells. The CFD was calculated for each condition by determining the line width required to achieve an intermediate level of sliding.